

Time Reversal Invariant Topological Superconductivity and Majorana Kramers Pairs

Fan Zhang,* C. L. Kane, and E. J. Mele

Department of Physics and Astronomy, University of Pennsylvania, Philadelphia, PA 19104, USA

We propose a feasible route to engineer one and two dimensional time reversal invariant (TRI) topological superconductors (SC) via proximity effects between nodeless s_{\pm} wave iron-based SC and semiconductors with large Rashba spin-orbit interactions. At the boundary of a TRI topological SC, there emerges a Kramers pair of Majorana edge (bound) states. For a Josephson π -junction we predict a Majorana quartet that is protected by mirror symmetry and leads to a mirror fractional Josephson effect. We analyze the evolution of Majorana pair in Zeeman fields, as the SC undergoes a symmetry class change as well as topological phase transitions, providing an experimental signature in tunneling spectroscopy. We briefly discuss the realization of this mechanism in candidate materials and the possibility of using s and d wave SC and weak topological insulators.

PACS numbers: 74.45.+c, 71.70.Ej, 71.10.Pm, 74.78.Na, 73.22.Gk, 74.78.Fk

Introduction.— Broken symmetry and topological order are two fundamental themes of condensed matter physics. The search for topological superconductors (SC) [1–3] is fascinating, as gauge symmetries are spontaneously broken in the bulk and gapless Andreev bound states (ABS) can be topologically protected at order parameter defects, hosting Majorana fermions. Majoranas are immune to local noise by virtue of their nonlocal topological nature and thus give hope for fault-tolerant quantum computing [4]. The rise of topological superconductivity (SC) has been expedited by recent proposals [5–9] that hybridize ordinary SC's with helical materials, with the help of magnetic perturbations. Using proximity effects, electrons in a single helical band at the Fermi energy form conventional Cooper pairs, whose condensation realizes a spinless chiral p wave SC in its weak pairing regime, *i.e.*, a topological SC with *broken* time reversal symmetry (class D). Unique signatures, including zero bias conductance peaks, anomalous Fraunhofer patterns, and fractional Josephson effects, are starting to be observed in these systems [10–14]. A completely distinct family (class DIII) of time reversal invariant (TRI) topological SC's was proposed based on a mathematical classification of Bogoliubov-de Gennes (BdG) Hamiltonians [15–20]. $\text{Cu}_x\text{Bi}_2\text{Se}_3$ [20] and Rashba bilayers [21] are possible candidates, if a fully gapped inter-orbital spin-triplet pairing dominates. This seems challenging since exotic interactions are required. Experimentally [22–27], the nature of the pairing remains very controversial.

A more ambitious goal is to realize TRI topological SC *without* exotic electron-electron interactions and *without* magnetic fields. Here we propose a feasible route to utilize proximity effect devices which combine Rashba semiconductors (RS) and *nodeless* iron-based SC's. Below its transition temperature the SC provides the RS a s_{\pm} wave spin-singlet pairing potential that switches sign between the Γ and M points [28–30]. TRI topological SC is realized when the chemical potential is adjusted to make the inner and outer Fermi surfaces feel pairing potentials with opposite signs. At a boundary of the 2D (1D)

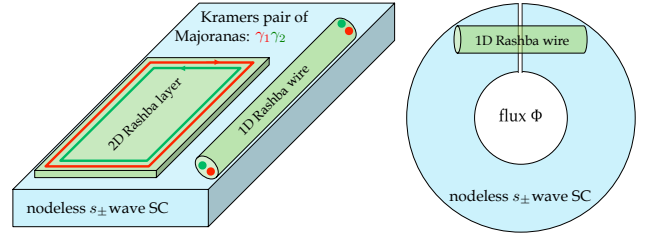


FIG. 1. Left panel: sketch of the proximity devices proposed in the text. A Majorana Kramers pair emerges at the boundary when the TRI SC becomes topological. Right panel: sketch of the Josephson junction described in the text.

TRI topological SC, a Kramers *pair* of Majorana edge (bound) states emerge as localized midgap states. For a Josephson π -junction a Majorana *quartet* is protected by mirror symmetry, leading to a *mirror* fractional Josephson effect. We analyze how the Majorana pair evolves in Zeeman fields, as the SC undergoes a symmetry class change and topological phase transitions, providing an experimental signature in tunneling spectroscopy.

2D TRI topological SC.— We first introduce a minimal model on a square lattice to characterize 2D TRI SC:

$$H = -t \sum_{\langle ij \rangle, \sigma} c_{i\sigma}^\dagger c_{j\sigma} - i\lambda_R \sum_{\langle ij \rangle} c_{i\alpha}^\dagger (\boldsymbol{\sigma}_{\alpha\beta} \times \hat{\mathbf{d}}_{ij})_z c_{j\beta} + \Delta_0 \sum_i (c_{i\uparrow}^\dagger c_{i\downarrow}^\dagger + \text{h.c.}) + \Delta_1 \sum_{\langle ij \rangle} (c_{i\uparrow}^\dagger c_{j\downarrow}^\dagger + \text{h.c.}). \quad (1)$$

Here t is the nearest neighbor hopping and $\boldsymbol{\sigma}$ are the Pauli matrices of electron spin. The second term arises from the Rashba spin-orbit interactions. Note that $\hat{\mathbf{d}}_{ij}$ is a unit vector pointing from site j to site i and we assume $\lambda_R > 0$. Δ_0 and Δ_1 , induced by the proximity effect, lead to a combined s_{\pm} wave pairing potential. It is more convenient to write the BdG Hamiltonian:

$$\begin{aligned} \mathcal{H}_{\mathbf{k}}^{\text{BdG}} &= [-2t(\cos k_x + \cos k_y) + h_{\mathbf{k}}^R - \mu] \tau_z + \Delta_{\mathbf{k}} \tau_x \\ h_{\mathbf{k}}^R &= 2\lambda_R(\sin k_x \sigma_y - \sin k_y \sigma_x) \\ \Delta_{\mathbf{k}} &= \Delta_0 + 2\Delta_1(\cos k_x + \cos k_y), \end{aligned} \quad (2)$$

where μ is the chemical potential and τ are the Pauli matrices in Nambu particle-hole notation. $\Delta_{\mathbf{k}}$ is a s_{\pm} wave singlet pairing potential that switches signs between the zone center Γ (0,0) and the zone corner M (π, π) when the order parameters satisfy $|\Delta_0| < 4|\Delta_1|$. As we show in Fig. 1(a) and note below, $\Delta_{\mathbf{k}}$ could be provided by a nodeless iron-based SC on which the Rashba layer is deposited. For convenience we have chosen a gauge to pin the overall phase of s_{\pm} wave SC at zero and assumed $0 < |\Delta_0| < 4\Delta_1$ hereafter. $\mathcal{H}_{\mathbf{k}}^{\text{BdG}}$ has time reversal ($\Theta = -i\sigma_y K$) and intrinsic particle-hole ($\Xi = \sigma_y \tau_y K$) symmetries. We obtain the energy dispersion

$$E_{\mathbf{k}}^{\text{BdG}} = \pm \sqrt{[2t(\cos k_x + \cos k_y) + \mu \pm \epsilon_{\mathbf{k}}^{\text{R}}]^2 + \Delta_{\mathbf{k}}^2}, \quad (3)$$

where $\epsilon_{\mathbf{k}}^{\text{R}} = 2\lambda_{\text{R}}\sqrt{\sin^2 k_x + \sin^2 k_y}$ is the Rashba energy. $\Delta_{\mathbf{k}}$ has a closed nodal line, *i.e.*, $\cos k_x + \cos k_y = -\Delta_0/(2\Delta_1)$, in the first Brillouin zone. At the nodal line, $E_{\mathbf{k}}^{\text{BdG}} = \pm(\mu - \epsilon_0 \pm \epsilon_{\mathbf{k}}^{\text{R}})$ with $\epsilon_0 = t\Delta_0/\Delta_1$, and $\epsilon_{\mathbf{k}}^{\text{R}}$ has the maxima $\epsilon_{\text{max}}^{\text{R}} = 2\lambda_{\text{R}}\sqrt{2 - \Delta_0^2/(8\Delta_1^2)}$ and the minima $\epsilon_{\text{min}}^{\text{R}} = 2\lambda_{\text{R}}\sqrt{|\Delta_0/\Delta_1| - \Delta_0^2/(4\Delta_1^2)}$.

In both 2D and 1D, the \mathbb{Z}_2 topological invariant [15–18] of a TRI SC is determined by whether the pairing potential has a negative sign on odd number of Fermi surfaces each of which encloses a TRI momentum [17]. As shown in Fig. 2 and summarized in Table I [31], the phase of the hybrid SC depends on the chemical potential μ . For the case of $\epsilon_{\text{min}}^{\text{R}} \leq |\mu - \epsilon_0| \leq \epsilon_{\text{max}}^{\text{R}}$, $\mathcal{H}_{\mathbf{k}}^{\text{BdG}}$ describes a nodal SC. When $|\mu - \epsilon_0| > \epsilon_{\text{max}}^{\text{R}}$, the SC is fully gapped but in the trivial ($\nu = 0$) phase since $\Delta_{\mathbf{k}}$ has the same sign on both Fermi circles. When $|\mu - \epsilon_0| < \epsilon_{\text{min}}^{\text{R}}$ is satisfied, the pairing potential switches sign between the two Fermi circles [32], and consequently the hybrid system realizes a TRI topological SC ($\nu = 1$). The energy window for tuning the system into the $\nu = 1$ state has the size of $2\epsilon_{\text{min}}^{\text{R}}$ with an optimized value $4\lambda_{\text{R}}$ at $\Delta_0 = \pm 2\Delta_1$. For the $\nu = 1$ state helical Majorana edge states emerge at the boundary, as shown in Fig. 2, the spectrum of a infinite ribbon described by Eq. (1). The Majoranas at $k = \pi$ (0) for $\text{sgn}(\Delta_0/\Delta_1) = 1$ (−1) are protected by time reversal and particle-hole symmetries.

1D TRI topological SC.— By turning off all the k_y terms Eq. (2) models a 1D Rashba nanowire deposited on a nodeless s_{\pm} wave SC. When the two s_{\pm} wave order parameters satisfy $|\Delta_0| < 2\Delta_1$, the pairing potential

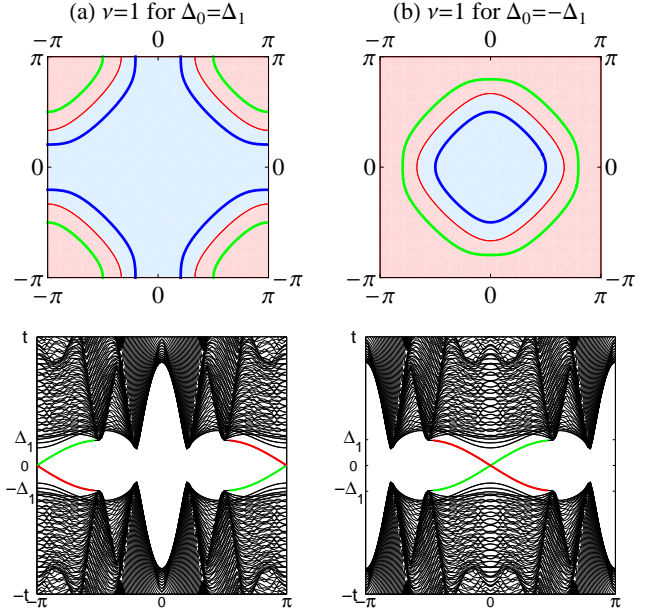


FIG. 2. Upper panels: the two Fermi surfaces (blue and green) of the single-particle bands for the $\nu = 1$ state; the closed nodal line (red) of $\Delta_{\mathbf{k}}$, separating two regions in which $\Delta_{\mathbf{k}}$ has opposite signs. Lower panel: BdG spectrum of a 2D ribbon as a function of k for the $\nu = 1$ state with $\mu = \epsilon_0$. The red and green lines indicate the helical Majorana edge states. We choose parameter values: $t = 10$, $\lambda_{\text{R}} = 5$, and $|\Delta_0| = \Delta_1 = 2$. (a) $\Delta_0 > 0$ and (b) $\Delta_0 < 0$.

switches sign between the two TRI momenta 0 and π . In 1D, the closed nodal line of $\Delta_{\mathbf{k}}$ is shrunk to two nodes at $k = \pm \arccos(-\Delta_0/2\Delta_1)$. At the nodes, the Rashba energy is $\epsilon_m^{\text{R}} = 2\lambda_{\text{R}}\sqrt{1 - \Delta_0^2/(4\Delta_1^2)}$, and thus a proximity induced 1D TRI nodal SC is identified for $\mu = \epsilon_0 \pm \epsilon_m^{\text{R}}$. When $|\mu - \epsilon_0| < \epsilon_m^{\text{R}}$, a positive pairing is induced for the inner pair of Fermi points while a negative pairing for the outer pair, realizing a 1D TRI topological SC. In the case of $|\mu - \epsilon_0| > \epsilon_m^{\text{R}}$, the hybrid system becomes a trivial SC that is adiabatically connected to the vacuum state.

At each end of a 1D TRI topological SC, there emerges a Kramers pair of Majorana bound states (MBS). Without loss of generality, in the rest of this paper we will set $\Delta_0 = 0$ for the 1D case and thus $|\mu| < 2\lambda_{\text{R}}$ is the criterion for the $\nu = 1$ state, as shown in Fig. 3(a). The cyan line denotes four degenerate MBS's independent of Δ_1 . Further investigation of their wavefunctions shows that these four MBS's form two Kramers pairs localized at the opposite ends of nanowire. This verifies our analytical results summarized in Table I.

Mirror Fractional Josephson effect.— Consider the linear Josephson junction in Fig. 1(b), in which a Rashba nanowire is deposited on a larger s_{\pm} wave SC ring, and the phase difference $\phi = (2e/\hbar)\Phi$ across the junction is controlled by the magnetic flux Φ through the ring. Fig. 3(b) shows the spectrum of ABS's as a function of ϕ

TABLE I. Summary of the \mathbb{Z}_2 classification of the hybrid TRI SC in class DIII. ϵ_0 , ϵ_m^{R} , $\epsilon_{\text{min}}^{\text{R}}$, and $\epsilon_{\text{max}}^{\text{R}}$ are defined in the text.

Phase	Two Dimension	One Dimension
$\nu = 1$	$ \mu - \epsilon_0 < \epsilon_{\text{min}}^{\text{R}}$	$ \mu - \epsilon_0 < \epsilon_m^{\text{R}}$
Nodal	$\epsilon_{\text{min}}^{\text{R}} \leq \mu - \epsilon_0 \leq \epsilon_{\text{max}}^{\text{R}}$	$ \mu - \epsilon_0 = \epsilon_m^{\text{R}}$
$\nu = 0$	$ \mu - \epsilon_0 > \epsilon_{\text{max}}^{\text{R}}$	$ \mu - \epsilon_0 > \epsilon_m^{\text{R}}$

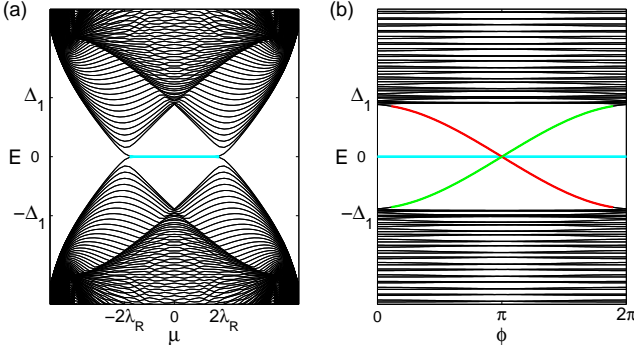


FIG. 3. (a) BdG spectrum of the 1D TRI SC as a function of μ . (b) Spectrum of ABS's in the junction as a function of ϕ . The cyan lines are four-fold degenerate, denoting two Kramers pairs of MBS's at opposite ends. The red and green lines are doubly degenerate, denoting two pairs of ABS's in the junction. We choose parameter values: $t = 10$, $\lambda_R = 5$, $\Delta_1 = 2$, and $\Delta_0 = 0$. $\mu = 0$ is used in (b).

when the physical separation between the ends of SC ring is small. The four-fold cyan line shows the appearance of a pair of MBS's at each end. The red and green lines, both doubly degenerate, represent two pairs of ABS's in the junction. When $\phi \neq \pi$, a finite μ lifts the degeneracy. However, protected by time reversal, particle-hole and mirror ($\mathcal{M}_y = -i\sigma_y$) symmetries, their crossing at $E = 0$ when $\phi = \pi$ is a four-fold degeneracy of special significance. This π -junction is in sharp contrast with its \mathbb{Z}_2 counterpart in the class without mirror symmetry [8, 18, 34]. Splitting the Majorana quartet at $\phi = \pi$ would break mirror and/or time reversal symmetry. To understand this topological twist in Fig. 3(b), we linearize Eq. (2) near the Fermi energy:

$$\mathcal{H}_{eff} = (vk_x\sigma_y - c)s\tau_z - \mu\tau_z + \mathcal{H}_{SC}, \quad (4)$$

$$\mathcal{H}_{SC} = \Delta s \left[\cos \frac{\phi}{2} \tau_x + \text{sgn}(x) \sin \frac{\phi}{2} \tau_y \right], \quad (5)$$

where $s = \pm$ denote the inner and outer bands with opposite spin helicities and c ($0 < c < \mu$) lifts their degeneracy [33]. The mirror symmetry allows one to label the bands with the eigenvalues of \mathcal{M}_y , $\alpha = \pm i$. We find the ABS dispersions $\epsilon_\alpha(\phi) = \Delta \cos(\phi/2)$. Note that the perfect normal state transmission and the independence on μ , c and α are artifacts of the simplified model. We can define Bogoliubov operators $\Gamma_{\alpha\pm}$ that satisfy $\Gamma_\alpha \equiv \Gamma_{\alpha+} = \Gamma_{\alpha-}^\dagger$ because of the particle-hole symmetry. The low-energy Hamiltonian is thus $H = \sum_\alpha \epsilon_\alpha(\phi) (\Gamma_\alpha^\dagger \Gamma_\alpha - \frac{1}{2}) = 2i \sum_\alpha \epsilon_\alpha(\phi) \gamma_\alpha \eta_\alpha$ where $\gamma_\alpha = (\Gamma_\alpha^\dagger + \Gamma_\alpha)/2$ and $\eta_\alpha = i(\Gamma_\alpha^\dagger - \Gamma_\alpha)/2$ are the Majorana operators. For each band, $N_\alpha^0 = \Gamma_\alpha^\dagger \Gamma_\alpha = 0, 1$ distinguishes two states and coupling them requires a process that changes N_α^0 . Due to the Cooper pairing, the total charge is not conserved. However, the fermion parity of each band $N_\alpha \bmod 2$ is conserved, as the mirror symmetry does not allow scattering between the two

bands. This *mirror fermion parity* conservation forbids the mixing among the four ABS's in the junction and therefore protects their crossing at zero energy. ϕ acts like a defect and parameterizes the mirror fermion parity pump. Although Eq. (4) is invariant under $\delta\Phi = h/2e$, the global Hamiltonian is physically distinct. When a flux $h/2e$ is threaded through the SC ring, ϕ is advanced by 2π , $\gamma_\alpha \rightarrow \gamma_\alpha$ while $\eta_\alpha \rightarrow -\eta_\alpha$, and a unit of fermion parity is transferred between the two bands resolving the fermion parity anomaly for an individual band.

In response to the change of phase, the populated ABS's carry supercurrents $I_{\alpha\pm} = \pm I_\alpha$ through the device, whereas the states in the continuum has negligible contributions. For the $\nu = 1$ case, we obtain $I_\alpha = (2e/h) \partial \epsilon_\alpha / \partial \phi = (-e\Delta/h) \sin(\phi/2)$, which is maximized at $\phi = \pi$ in sharp contrast to the $\nu = 0$ (conventional) case. In the absence of mirror symmetry breaking, there is no transition among $I_{\alpha\pm}$, signaling a mirror fractional Josephson effect with 4π periodicity.

Evolution of Majorana pair in Zeeman field.— When one helical band is removed from the Fermi energy, a Rashba nanowire proximity coupled to a s wave SC is a topological SC with broken time reversal symmetry, supporting a single MBS at each end. Realizing such a topological phase requires the Zeeman field $V_z\sigma_z$ (or $V_z\sigma_x$) and the chemical potential μ to satisfy: $4\Delta_1^2 + (|\mu| - 2t)^2 < V_z^2 < 4\Delta_1^2 + (|\mu| + 2t)^2$. Since only one helical band is present at the Fermi energy this also occurs even if the SC is s_\pm wave as long as the hybrid SC remains fully gapped ($\mu^2 \neq 4\lambda_R^2 + V_z^2$). The latter condition is guaranteed for the TRI $\nu = 1$ state as it satisfies $|\mu| < 2\lambda_R$. It is thus intriguing to investigate how a MBS pair evolves in the Zeeman field, as the bulk SC undergoes a symmetry class change and topological phase transitions. Fig. 4(a) shows the evolution in the case of $\mu \neq 0$. When V_z is turned on, without gap closing, the topological SC in the TRI class becomes a trivial SC in the class without time reversal symmetry. Two topological phase transitions occur at $V_z^2 = 4\Delta_1^2 + (|\mu| \pm 2t)^2$ where the gap closes. The $\nu = 1$ state in the new class is realized between the transitions. At one end, as V_z is tuned up, one MBS disappears at the first transition while the other persists in the $\nu = 1$ state and enters the bulk continuum at the second transition. For the special case $\mu = 0$, the two transitions merge into one and the new $\nu = 1$ state does not appear.

As implied by the zero energy black lines in Fig. 4(a), it seems baffling that the Majorana pair is robust against the Zeeman field before the first transition occurs. We emphasize that these Majoranas are not topologically protected because the bulk SC is trivial in the new class. However, their robustness can be understood using the effective model described by Eq. (4) with

$$\mathcal{H}_{SC} = \Delta s \tau_x \theta(a - |x|) + \bar{\Delta} \tau_x \theta(|x| - a), \quad (6)$$

where $x = \pm a$ are the locations of the two ends of SC and $\bar{\Delta} \rightarrow \infty$ reflects the infinity mass of vacuum. Eq. (6)

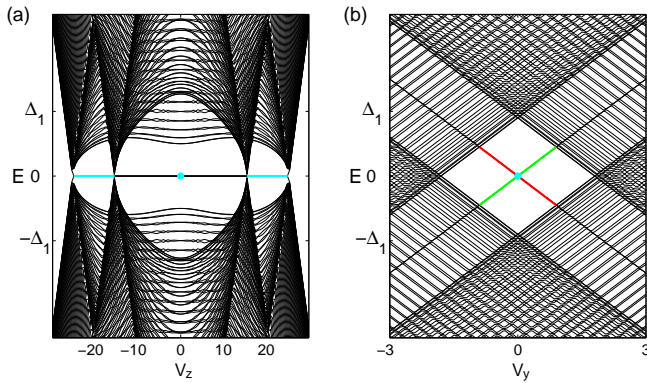


FIG. 4. Evolution of a MBS pair in Zeeman fields. (a) In a σ_z (σ_x) field; (b) in a σ_y field. The cyan dots (lines) have two-fold (no) degeneracy, indicating the appearance of a MBS pair (single MBS) at the end of SC. The black lines at zero energy are doubly degenerate. The red and green lines indicate the Zeeman splitting of two zero energy states with opposite fermion parity. We choose parameter values: $\mu = -5$ in (a), $\mu = 0$ in (b), and others are the same as in Fig. 3.

incorporates the correct boundary condition [35] of TRI topological SC. Solving the boundary problem, we find that a pair of MBS's at one end forms two states with $\sigma_y = \tau_y = \pm 1$ while the other pair at the opposite end forms two states with $\sigma_y = -\tau_y = \pm 1$. Clearly, a σ_x or σ_z Zeeman field only couples states with opposite σ_y flavors at opposite ends, whose wavefunction overlap decays exponentially on the SC length. Consequently, none of the Majoranas can be passivated away from zero energy until the first topological phase transition. However, as shown in Fig. 4(b), a small σ_y field can Zeeman split the two zero energy states with opposite fermion parity at each end, revealing the topological triviality of bulk SC. The σ_y field also closes the SC gap.

The evolution of a Majorana pair in a Zeeman field provides a smoking gun for the identification of a TRI topological SC in tunneling spectroscopy. The Majorana pair induces resonant Andreev reflection producing a zero bias conductance peak [36–38] of $4e^2/h$. This peak persists for small σ_x and σ_z fields, reduces to $2e^2/h$ after the first topological quantum phase transition, and disappears at the second one. In contrast, a small σ_y field not only Zeeman splits but also reduces the peak.

Discussions.— Unlike a d_{xy} wave SC, where it is impossible to induce a full gap at the Fermi surface centered at a TRI momentum, a nodeless s_{\pm} or $d_{x^2-y^2}$ wave SC allows the pairing potentials on Fermi surfaces centered at $(0, 0)$ and (π, π) or at $(0, \pi)$ and $(\pi, 0)$ to have opposite signs. Therefore, it would be interesting to consider 2D TRI topological SC in a proximity device that hybridize a *weak* topological insulator with two surface states and a *nodeless* s_{\pm} or $d_{x^2-y^2}$ wave SC [31]. Although the rotational symmetry of RS makes the hybrid 2D $d_{x^2-y^2}$ wave SC nodal, it is still possible to use them to engineer

a 1D TRI topological SC. This has been recently suggested by Wong and Law [39], however, the $d_{x^2-y^2}$ wave heavy fermion SC they chose is nodal, which provides a decay channel for MBS's and destroys their topological robustness. One may also wonder whether it is possible to build a hybrid TRI topological SC using a s wave SC if the proximity effect is strongly orbital-dependent. Unfortunately, this seems not plausible for the reason that we elaborate in the supplementary materials [31].

Our proposal is experimentally feasible, since the necessary ingredients and the required technologies are all well established. It has been widely accepted that, at least for iron pnictides, there are a large family of nodeless s_{\pm} wave SC's [28–30], though their pairing mechanism is still under lively debate. An iron-pnictide with closer electron and hole Fermi surfaces is preferred. $\Delta_{0,1}$ can be adjusted by doping or changing materials. Iron-pnictides consist of square layers that are stacked in tetragonal structures and it is better to choose RS with cubic or tetragonal crystal structures, *e.g.*, Au, Ag and Pb, in order to match their Brillouin zones (BZ). A small lattice incommensurability may blur and thus effectively broaden the pairing potential in the BZ of RS, which may even be helpful as long as the SC remains nodeless.

Our proposal for a realization of TRI topological SC's in 1D and 2D constitutes four critical advances: (i) there is no need for magnetic perturbations or exotic interactions, simplifying the experimental setup; (ii) the SC gap can reach more than 15 meV, raising the critical temperature of topological SC; (iii) it is likely that the presence of time reversal symmetry mitigate the role of disorder via Anderson's Theorem, making the topological SC even more robust; and (iv) irrelevant bands [40] are completely absent, allowing large tunability in feasible materials.

Acknowledgements.— This work has been supported by DARPA grant SPAWAR N66001-11-1-4110. CLK has been supported by NSF grant DMR 0906175 and a Simons Investigator award from the Simons Foundation.

* zhf@sas.upenn.edu

- [1] N. Read and D. Green, Phys. Rev. B **61**, 10267 (2000).
- [2] D. A. Ivanov, Phys. Rev. Lett. **86**, 268 (2001).
- [3] A. Kitaev, Phys. Usp. **44** (suppl.), 131 (2001); Ann. Phys. (N.Y.) **303**, 2 (2003).
- [4] C. Nayak, S. H. Simon, A. Stern, M. Freedman, and S. Das Sarma, Rev. Mod. Phys. **80**, 1083 (2008).
- [5] L. Fu and C. L. Kane, Phys. Rev. Lett. **100**, 096407 (2008).
- [6] J. D. Sau, R. M. Lutchyn, S. Tewari, and S. Das Sarma, Phys. Rev. Lett. **104**, 040502 (2010).
- [7] J. Alicea, Phys. Rev. B **81**, 125318 (2010).
- [8] R. M. Lutchyn, J. D. Sau, S. Das Sarma, Phys. Rev. Lett. **105**, 077001 (2010).
- [9] Y. Oreg, G. Refael, and F. von Oppen, Phys. Rev. Lett. **105**, 177002 (2010).

- [10] V. Mourik, K. Zuo, S. M. Frolov, S. R. Plissard, E. P. A. M. Bakkers, and L. P. Kouwenhoven, *Science* **25**, 1003-1007 (2012).
- [11] M. T. Deng, C. L. Yu, G. Y. Huang, M. Larsson, P. Caroff, and H. Q. Xu, *Nano Lett.* **12**, 6414 (2012).
- [12] M. Veldhorst, M. Snelder, M. Hoek, T. Gang, V. K. Guduru, X. L. Wang, U. Zeitler, W. G. van der Wiel, A. A. Golubov, H. Hilgenkamp, and A. Brinkman *Nature Materials* **11**, 417 (2012).
- [13] J. R. Williams, A. J. Bestwick, P. Gallagher, S. S. Hong, Y. Cui, A. S. Bleich, J. G. Analytis, I. R. Fisher and D. Goldhaber-Gordon, *Phys. Rev. Lett.* **109**, 056803 (2012).
- [14] L. P. Rokhinson, X. Liu, and J. K. Furdyna, *Nature Physics* **8**, 795 (2012).
- [15] A. P. Schnyder, S. Ryu, A. Furusaki, and A. W. W. Ludwig, *Phys. Rev. B* **78**, 195125 (2008).
- [16] A. Kitaev, arXiv:0901.2686 (2009); *AIP Conf. Proc.* **1134**, 22 (2009).
- [17] X. Qi, T. L. Hughes, and S. Zhang, *Phys. Rev. B* **81**, 134508 (2010).
- [18] J. Teo and C. L. Kane, *Phys. Rev. B* **82** 115120 (2010). The fermion parity pump corresponds to the entry with a reduced dimension $\delta = d - D = 0$ in Tabel I of Ref. 18.
- [19] M. Sato, *Phys. Rev. B* **81**, 220504(R) (2010).
- [20] L. Fu and E. Berg, *Phys. Rev. Lett.* **105**, 097001 (2010).
- [21] S. Nakosai, Y. Tanaka, and N. Nagaosa, *Phys. Rev. Lett.* **108**, 147003 (2012).
- [22] Y. S. Hor, A. J. Williams, J. G. Checkelsky, P. Roushan, J. Seo, Q. Xu, H. W. Zandbergen, A. Yazdani, N. P. Ong, and R. J. Cava, *Phys. Rev. Lett.* **104**, 057001 (2010).
- [23] L. A. Wray, S. Y. Xu, Y. Xia, Y. S. Hor, D. Qian, A. V. Fedorov, H. Lin, A. Bansil, R. J. Cava, and M. Z. Hasan, *Nature Phys.* **6**, 855 (2010).
- [24] S. Sasaki, M. Kriener, K. Segawa, K. Yada, Y. Tanaka, M. Sato, and Y. Ando, *Phys. Rev. Lett.* **107**, 217001 (2011).
- [25] T. Kirzhner, E. Lahoud, K. B. Chaska, Z. Salman, and A. Kanigel, *Phys. Rev. B* **86**, 064517 (2012).
- [26] X. Chen, C. Huan, Y. S. Hor, C. A. R. Sá de Melo, and Z. Jiang arXiv:1210.6054 (2012).
- [27] N. Levy, T. Zhang, J. Ha, F. Sharifi, A. A. Talin, Y. Kuk, and J. A. Stroscio, arXiv:1211.0267 (2012).
- [28] K. Ishida, Y. Nakai, and H. Hosono, *J. Phys. Soc. Jpn.*, **78**, 062001 (2009).
- [29] I. I. Mazin, *Nature* **464**, 183 (2010).
- [30] We only use the nodeless s_{\pm} wave iron-based SC's, *i.e.*, iron-pnictides, single-layer iron-chalcogenides but not double-layer iron-chalcogenides; T. Das and A. V. Balatsky, *J. Phys.: Condens. Matter* **24**, 182201 (2012).
- [31] See the supplementary materials.
- [32] When λ_R is too large (which is not realistic), there could be two extra small Fermi circles at $(0, \pi)$ and $(\pi, 0)$ for some parameter values. Because the s_{\pm} wave pairing potential is guaranteed to have the same sign on these two Fermi surfaces, there is no influence.
- [33] This $cs\tau_z$ term also indicates the broken inversion symmetry of the Rashba system.
- [34] L. Fu and C. L. Kane, *Phys. Rev. B* **79**, 161408(R) (2009).
- [35] F. Zhang, C. L. Kane, and E. J. Mele, *Phys. Rev. B* **86**, 081303(R) (2012).
- [36] K. T. Law, P. A. Lee, and T. K. Ng, *Phys. Rev. Lett.* **103**, 237001 (2009).
- [37] M. Wimmer, A. R. Akhmerov, J. P. Dahlhaus, and C. W. J. Beenakker, *New J. Phys.* **13**, 053016 (2011).
- [38] For a review see: C. W. J. Beenakker, arXiv:1112.1950 (2011).
- [39] L. M. Wong and K. T. Law, arXiv:1211.0338 (2012).
- [40] The bulk bands [5] or the helical band removed from the Fermi energy [6–9] plays negative roles in realizing a class D topological SC experimentally.

Supplementary Materials

Fan Zhang,* E. J. Mele, and C. L. Kane

Department of Physics and Astronomy, University of Pennsylvania, Philadelphia, PA 19104, USA

PACS numbers: 74.45.+c, 71.70.Ej, 71.10.Pm, 74.78.Na, 73.22.Gk, 74.78.Fk

I. 2D time reversal invariant topological Superconductivity

We further illustrate the 2D \mathbb{Z}_2 classification described in the main text and summarized in Table I. The energy dispersion at the nodal line of pairing potential reads

$$E_{\mathbf{k}}^{\text{BdG}} = \pm (\mu - \epsilon_0 \pm \epsilon_{\mathbf{k}}^{\text{R}}), \quad (1)$$

where $\epsilon_{\mathbf{k}}^{\text{R}}$ is the energy associated with the Rashba spin-orbit couplings. At the nodal line, $\epsilon_{\mathbf{k}}^{\text{R}}$ has the maxima $\epsilon_{\text{max}}^{\text{R}} = 2\lambda_{\text{R}}\sqrt{2 - \Delta_0^2/(8\Delta_1^2)}$ and the minima $\epsilon_{\text{min}}^{\text{R}} = 2\lambda_{\text{R}}\sqrt{|\Delta_0/\Delta_1| - \Delta_0^2/(4\Delta_1^2)}$. The lower panel of Fig. 1 depicts the energy dispersions of the two single-particle bands at the nodal line of pairing potential. (i) For the case of $\epsilon_{\text{min}}^{\text{R}} \leq |\mu - \epsilon_0| \leq \epsilon_{\text{max}}^{\text{R}}$, $\mathcal{H}_{\mathbf{k}}^{\text{BdG}}$ describes a nodal superconductor, as Eq. (1) can be zero for some momenta. (ii) When $|\mu - \epsilon_0| > \epsilon_{\text{max}}^{\text{R}}$, the superconductor is fully gapped but in the trivial ($\nu = 0$) phase, because $\Delta_{\mathbf{k}}$ has the same sign at both Fermi circles. (iii) Only when $|\mu - \epsilon_0| < \epsilon_{\text{min}}^{\text{R}}$ is satisfied, the pairing potential switches sign between the two Fermi circles, and consequently the hybrid system realizes the time reversal invariant topological superconductivity ($\nu = 1$).

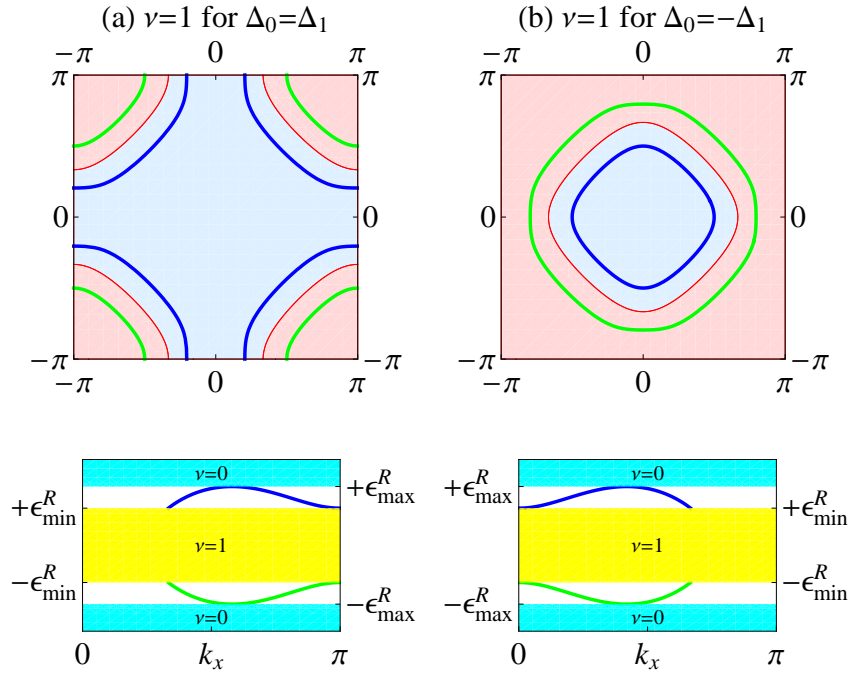


FIG. 1: Upper panels: the two Fermi surfaces (blue and green) of the single-particle bands for the $\nu = 1$ state; the closed nodal line (red) of $\Delta_{\mathbf{k}}$ separating two regions in which $\Delta_{\mathbf{k}}$ has opposite signs. Lower panels: the energy dispersions of the two single-particle bands at the nodal line of $\Delta_{\mathbf{k}}$ in the region $0 \leq k_x \leq \pi/2$ and $k_y \geq 0$, where ϵ_0 is defined as the energy origin; μ lies in yellow, cyan and white regions correspond to $\nu = 1$, $\nu = 0$ and nodal states in Table I.

II. Using a weak topological insulator

A nodeless s_{\pm} or $d_{x^2-y^2}$ wave superconductor allows the pairing potentials on Fermi surfaces centered at $(0,0)$ and (π,π) or at $(0,\pi)$ and $(\pi,0)$ to have opposite signs. Therefore, it is promising to build 2D time reversal invariant topological superconductivity in a proximity device that hybridize a weak topological insulator with two surface states and a *nodeless* s_{\pm} or $d_{x^2-y^2}$ wave superconductor. This two possibilities are sketched in Fig. 2.

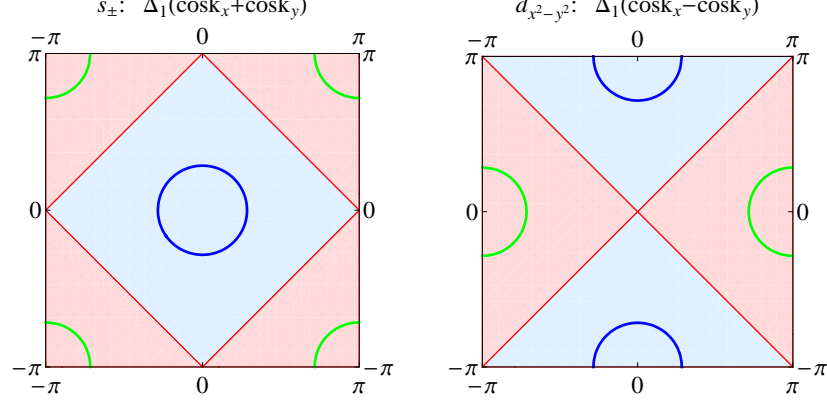


FIG. 2: In each panel, the blue and green circles denote two Fermi surfaces of the surface state of a weak topological insulator, and the red line separates two regions in which $\Delta_{\mathbf{k}}$ has opposite signs.

III. Possibility of using a s wave superconductor

To elaborate this point, we use Eq. (4) with $c = 0$ and s replaced by s_z . $s_z = \pm 1$ denote the top/bottom surface state (or layer) in the case of strong topological insulators (ref. 35) or bilayer Rashba films (ref. 24). $ms_x\tau_z$ can be understood as a small *trivial* gap at $k = 0$ due to the tunneling between the (top-or-bottom) orbital-pseudospins. In the weak tunneling limit, the proximity induced pairing potential has the form of

$$T\tau_x = [(t_T^2 + t_B^2)/2 + (t_T^2 - t_B^2)/2 s_z + t_T t_B s_x] \tau_x, \quad (2)$$

where t_T (t_B) is the tunneling amplitude between the superconductor and the top (bottom) orbital. We have assumed t_T and t_B are real without loss of generality, and will use $T_{I,z,x}$ to denote the three coefficients quadratic in t in the bracket. Note that only the $s_z\tau_x$ pairing, breaking inversion symmetry, gives rise to the topological superconducting state in class DIII. However, such a state will compete with the trivial superconducting state. Focusing on \mathcal{H}_{SC} , the superconducting gap is proportional to $|T_I - \sqrt{T_x^2 + T_z^2}|$ which vanishes. Therefore the hybrid superconductor is nodal. Even if the inter-orbital pairing is not allowed, *i.e.*, $T_x = 0$, $T_I > |T_z|$ is generally valid and therefore pins the hybrid superconductor to the trivial state. When the s wave superconductor is integrated out in the standard second order perturbation theory, the renormalized pairing potential reads

$$\tilde{\Delta} = \frac{\Gamma_N \Delta}{\sqrt{\Delta^2 - \omega^2}} \det^{-1} \left(1 + \frac{\Gamma_N}{\sqrt{\Delta^2 - \omega^2}} \right) \quad (3)$$

with $\Gamma_N = \pi N_0 V T$. Here V and N_0 are the tunneling volume and the density of states of the superconductor in the normal state at the Fermi energy. Interestingly and obviously, the conclusions are unchanged at the Fermi energy in this more rigorous approach. Similar analysis and conclusions can be generalized to the case with both orbital and spin flavors, in which the spin-triplet pairing $\sigma_z s_y \tau_x$ leads to a topological state.

* Electronic address: zhf@sas.upenn.edu